Control of unstable steady states by long delay feedback

Serhiy Yanchuk,[1,2] Matthias Wolfrum,[1] Philipp Hövel,[3] and Eckehard Schöll[3]
[1]*Weierstrass Institute for Applied Analysis and Stochastics, 10117 Berlin, Germany*
[2]*Institute of Mathematics, Humboldt University of Berlin, Unter den Linden 6, 10099 Berlin, Germany*
[3]*Institut für Theoretische Physik, Technische Universität Berlin, 10623 Berlin, Germany*
(Received 11 April 2006; published 2 August 2006)

We present an asymptotic analysis of time-delayed feedback control of steady states for large delay time. By scaling arguments, and a detailed comparison with exact solutions, we establish the parameter ranges for successful stabilization of an unstable fixed point of focus type. Insight into the control mechanism is gained by analyzing the eigenvalue spectrum, which consists of a pseudocontinuous spectrum and up to two strongly unstable eigenvalues. Although the standard control scheme generally fails for large delay, we find that if the uncontrolled system is sufficiently close to its instability threshold, control does work even for relatively large delay times.

DOI: 10.1103/PhysRevE.74.026201 PACS number(s): 05.45.Gg, 02.30.Ks

I. INTRODUCTION

The stabilization of unstable and chaotic systems is the subject of extensive investigations in physics, chemistry, biology, and medicine [1–3]. Starting with the work of Ott, Grebogi, and Yorke [4], a variety of methods for chaos control have been developed in order to stabilize unstable periodic orbits (UPOs) embedded in a chaotic attractor. A particularly simple and efficient scheme is time-delayed feedback, which uses the difference $s(t)-s(t-\tau)$ of a signal s at a time t and a delayed time $t-\tau$ as suggested by Pyragas [5]. This method is noninvasive since the stabilized state exists already—though unstable—in the uncontrolled system, and the control force vanishes when a UPO of period τ is reached. This scheme was improved by Socolar *et al.* [6] by considering multiple delays in the form of an infinite series (*extended time-delay autosynchronization* or ETDAS), and other variants have also been elaborated [7–12]. Some analytical results on the conditions for control can be obtained from the Floquet spectrum of the UPOs [13–17], and a detailed numerical bifurcation analysis has been performed [18].

Time-delayed feedback with appropriate time delay can also be used to stabilize unstable steady states [19]. This scheme is more robust than derivative control of fixed points [20,21], and has been applied to electrochemical systems [22,23] and nonlinear electronic circuits [24]. All-optical realizations are another important application of time-delay autosynchronization. In particular, a time-delayed optical feedback occurs naturally in semiconductor lasers [25–28], and often the delay time is rather large [29,30]. Time-delayed feedback control of steady states has been studied in semiconductor lasers under resonant feedback from a Fabry-Perot resonator [31].

It is the purpose of this paper to obtain deeper analytical insight into the time-delayed feedback control of steady states for large delay by relating asymptotic properties of the eigenvalue spectrum with the exact solutions, and by discussing the shape of the control domain in the space of the control parameters. It has been shown that time-delayed feedback control fails if the number of positive eigenvalues of the fixed point (or more generally, positive Floquet exponents of the UPO) is odd [14,15], hence we consider an unstable fixed point of focus type with two complex-conjugate eigenvalues $\Lambda=\lambda\pm i\omega$, $\lambda>0$. If $\lambda\to 0$, a reverse Hopf bifurcation occurs, and the fixed point becomes stable. Three different time scales are of importance in such a control problem: (i) the inverse divergence rate of trajectories around the unstable fixed point $1/\lambda$, (ii) the period of undamped oscillations around the fixed point $T_0=2\pi/\omega$, where ω is the oscillation frequency, and (iii) the delay time τ used in the feedback control loop. Here we consider the case $\tau\gg 1/\lambda$, and study a generic model equation that describes an unstable focus above a Hopf bifurcation. The paper is organized as follows. In Sec. II, we present the analytical solution of the complex spectrum as a function of delay time using the Lambert function. In Sec. III, the scaling properties of the spectrum for large delay are derived. From this, the control domain close to the Hopf bifurcation of the fixed point is constructed (Sec. IV). The Appendix contains the explicit analytical form of the boundary of the control domain.

II. STABILIZATION OF AN UNSTABLE FIXED POINT

The stability of a fixed point $\mathbf{x}^*$ in a general nonlinear dynamic system is obtained by linearizing the vector field around $\mathbf{x}^*$. Hence, in order to study the stabilization of fixed points by time-delayed feedback control, it is sufficient to consider the generic model of a two-variable linear system that, in the absence of delay, has an unstable focus at $x^*=0$, $y^*=0$ with eigenvalues of the Jacobian $\lambda\pm i\omega$, $\lambda>0$, $\omega\neq 0$.

Applying the standard diagonal time-delayed feedback control scheme, we obtain the basic model equation for stabilizing unstable steady states [19],

$$\dot{x}(t)=\lambda x(t)+\omega y(t)-K[x(t)-x(t-\tau)],$$

$$\dot{y}(t)=-\omega x(t)+\lambda y(t)-K[y(t)-y(t-\tau)], \qquad (1)$$

where K is the feedback control strength, and τ is a feedback delay time. In the absence of control, the zero fixed point has

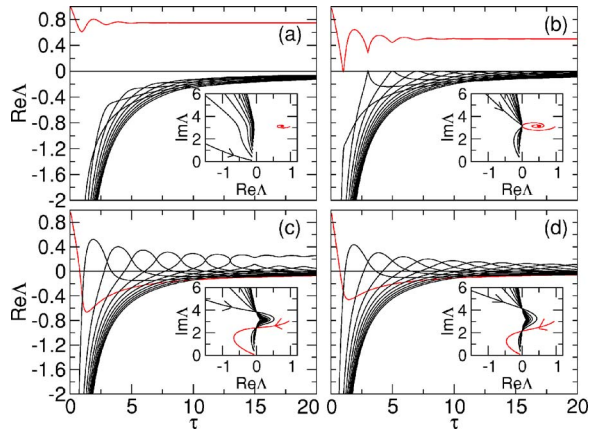

FIG. 1. (Color online) Real parts of the complex eigenvalues Λ as a function of τ calculated from the characteristic Eq. (2) for 10 modes with the largest real parts. (a) $K=0.25$, (b) $K=0.5$, (c) $K=0.75$, and (d) $K=1.0$. Inset: eigenmodes Λ in the complex plane for $\tau \in [0,20]$. Red curves: Eigenvalue originating from the uncontrolled system; black curves: eigenmodes created by the delay control. Parameters: $\omega=\pi$, $\lambda=1$.

the eigenvalues $\Lambda=\lambda\pm i\omega$, $\lambda>0$, i.e., the parameters $\lambda>0$ and ω are a measure for the distance from the instability threshold, e.g., a Hopf bifurcation, and the intrinsic eigenfrequency, respectively.

In the presence of the control, the stability of the fixed point is determined by the roots Λ of the characteristic equation

$$[\Lambda + K(1-e^{-\Lambda\tau}) - \lambda]^2 + \omega^2 = 0.$$

This equation can be further simplified to

$$\lambda \pm i\omega = \Lambda + K(1-e^{-\Lambda\tau}). \tag{2}$$

Note that due to the presence of the delay, Eq. (2) possesses infinitely many solutions. Nevertheless, the stability of the fixed point is determined by a finite number of critical roots with the largest real parts [32]. As a result, the stabilization problem consists in determining these critical eigenvalues and describing their behavior. In particular, successful control is achieved by providing conditions in terms of the control parameters K and τ for which all critical eigenvalues have negative real parts.

Using the Lambert function W, which is defined as the inverse function of $g(z)=ze^z$ for complex z [32], the solution of Eq. (2) can be expressed as

$$\Lambda\tau = W(K\tau e^{-(\lambda\pm i\omega)\tau+K\tau}) + (\lambda \pm i\omega)\tau - K\tau. \tag{3}$$

Figure 1 shows the real parts of the critical eigenvalues Λ as a function of τ for different values of K. The insets show the same eigenvalues as curves in the complex plane, parametrized by τ. Note that the eigenvalue originating from the uncontrolled system (red online) is the most unstable one for sufficiently small K and does not couple to the eigenvalues generated by the delay [see Figs. 1(a) and 1(b)]. The countable set of eigenvalues generated by the delay originates from $\mathrm{Re}\,\Lambda=-\infty$ for $\tau\to 0$, and shows the typical nonmonotonic behavior that leads to stability islands for appropriate τ and K [19]. For larger values of K, the eigenvalue originating from the uncontrolled system is no longer separated from those generated by the delay [see Figs. 1(c) and 1(d)]. Moreover, one can observe a scaling behavior of the real parts of the eigenvalues for large τ : in Figs. 1(a)–1(c), there is a single eigenvalue retaining a positive real part, whereas all the other real parts tend to zero for large τ. The insets show that the eigenvalues in fact accumulate along the imaginary axis. This observation will be studied in detail in the following section.

III. ASYMPTOTIC PROPERTIES OF THE SPECTRUM FOR LARGE DELAY

The scaling behavior of eigenvalues of general linear delay-differential equations for large delay τ has been analyzed in [33]. In particular, it turns out that one can distinguish the following.

(a) *Strongly unstable eigenvalues* Λ_s which have positive real parts that do not tend to zero with increasing τ, i.e., $\Lambda_s\to$const and $\mathrm{Re}\,\Lambda_s \geqslant \delta$ for some $\delta>0$ as $\tau\to\infty$.

(b) *Pseudocontinuous spectrum* (PS) of eigenvalues Λ_p with real parts that scale as $1/\tau$, i.e., $\Lambda_p=\frac{1}{\tau}\gamma+i\left(\Omega+\frac{1}{\tau}\varphi\right)+O\left(\frac{1}{\tau^2}\right)$ with some γ, Ω, and φ. A spectrum with this scaling behavior and positive real part leads to so-called *weak instabilities* (for more details, see [33,34]).

In order to obtain the strongly unstable eigenvalues, we insert $\Lambda_s=$const into Eq. (2) and assume $\tau\to\infty$. Since $\mathrm{Re}\,\Lambda_s>\delta$, the exponential term vanishes and we arrive at the expression for Λ_s:

$$\Lambda_s = \lambda - K \pm i\omega,$$

which holds for $\lambda-K>0$. Thus we obtain the following statement:

(i) For $K<\lambda$, there exist two eigenvalues of the controlled stationary state, Λ_{s1} and its complex-conjugate Λ_{s2}, such that $\Lambda_{s1}\to\lambda-K+i\omega$ as $\tau\to\infty$. The real parts of these eigenvalues are positive and, hence, the stationary state is *strongly unstable* [cf. Figs. 1(a)–1(c)].

In order to obtain the asymptotic expression for the remaining pseudocontinuous part of the spectrum, we have to insert the scaling $\Lambda_p=\frac{1}{\tau}\gamma+i\left(\Omega+\frac{1}{\tau}\varphi\right)$ into Eq. (2). Up to the leading order, we obtain the equation

$$i\Omega + K(1-e^{-\gamma}e^{-i\varphi}) = \lambda \pm i\omega, \tag{4}$$

and the additional condition $\Omega=\Omega^{(m)}=2\pi m/\tau$, $m=\pm 1,\pm 2,\pm 3,\ldots$. Equation (4) can be solved with respect to $\gamma(\Omega)$,

$$\gamma(\Omega) = -\frac{1}{2}\ln\left[\left(1-\frac{\lambda}{K}\right)^2 + \left(\frac{\Omega\pm\omega}{K}\right)^2\right]. \tag{5}$$

The fact that $\mathrm{Re}\,\Lambda_p \approx \gamma(\Omega)/\tau$ and $\mathrm{Im}\,\Lambda_p\approx\Omega$ up to the leading order means that the eigenvalues Λ_p accumulate in the complex plane along curves $(\gamma(\Omega),\Omega)$, provided that the real axis is scaled as $\tau\,\mathrm{Re}\,\Lambda$. The actual positions of the eigenvalues on the curves can be obtained by evaluating Ω at points $\Omega^{(m)}=2\pi m/\tau$. With increasing τ, the eigenvalues cover the curves densely [33]. Hence, we obtain the second statement:

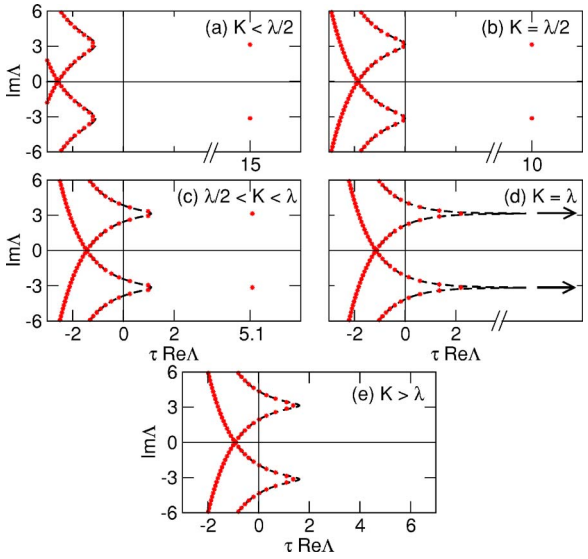

FIG. 2. (Color online) Numerically computed spectrum of eigenvalues for $\tau=20$ (asterisks, red online). The dashed lines depict the asymptotic pseudocontinuous spectrum. (a) Strong instability for $K=0.25$ $(K<\lambda/2)$; (b) $K=0.5=\lambda/2$, critical case at which the weak instability occurs in addition to the strong one; (c) $K=0.75$ $(\lambda/2<K<\lambda)$, strong and weak instability; (d) $K=1.0=\lambda$, critical case at which a strong instability disappears via the singularity of the pseudocontinuous spectrum; (e) $K=1.25$ $(K>\lambda)$, weak instability. Parameters: $\omega=\pi$, $\lambda=1$.

(ii) The fixed point of system (1) has a set of eigenvalues that behave asymptotically as $\Lambda_p(\Omega^{(k)})=\frac{1}{\tau}\gamma(\Omega^{(k)})+i\left[\Omega^{(k)}+\frac{1}{\tau}\varphi(\Omega^{(k)})\right]$ with $\gamma(\Omega)$ given by Eq. (5). We have *weak instability* if the maximum of $\gamma(\Omega)$ is positive, i.e.,

$$\gamma_{\max}=\max_{\Omega}\gamma(\Omega)=-\ln\left|1-\frac{\lambda}{K}\right|>0,$$

which is the case for $K>\lambda/2$.

Figure 2 illustrates the spectrum of the fixed point of system (1) for $\tau=20$. One can clearly distinguish the two types of eigenvalues. For $K<\lambda/2$ [Fig. 2(a)], the fixed point has a pair of strongly unstable eigenvalues, whereas the PS is stable. Note that the symbols (red online) show the spectrum computed numerically from the full eigenvalue equation, whereas the dashed lines are the curves $(\gamma(\Omega),\Omega)$ from the asymptotic approximation where the PS accumulates for large τ. At $K=\lambda/2$ [cf. Fig. 2(b)], the PS touches the imaginary axis resulting in the appearance of a weak instability for $K>\lambda/2$. This leads to the coexistence of strong and weak instabilities for $\lambda/2<K<\lambda$ [Fig. 2(c)]. At $K=\lambda$, the strongly unstable eigenvalues disappear, being absorbed by the PS, which develops a singularity at this moment, cf. Fig. 2(d). Finally, for $K>\lambda$ [Fig. 2(e)], there occurs only a weak instability induced by the PS.

After inspecting all possibilities given in Fig. 2, we conclude that stabilization by the feedback control scheme (1) always has an upper limit τ_c such that for $\tau>\tau_c$ it fails. Additionally, we note that for $K<\lambda$ and large delay, the stationary state is strongly unstable with the complex-conjugate eigenvalues $\Lambda_{1,2}=\lambda-K\pm i\omega$, and for $K>\lambda$ weakly unstable with a large number of unstable eigenvalues given by Eq. (4), the real parts of which scale as $1/\tau$.

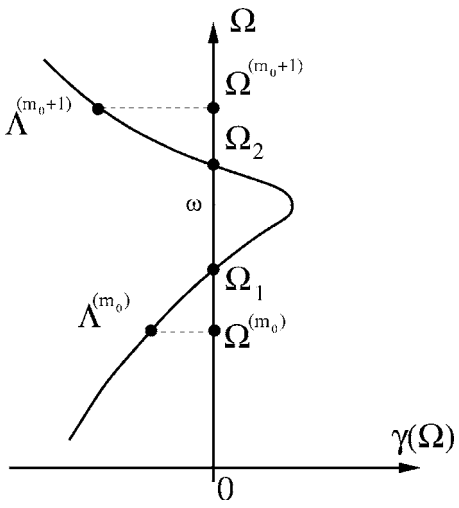

FIG. 3. Curve of the pseudocontinuous spectrum. The actual position of the complex eigenvalues $\Lambda=\frac{1}{\tau}\gamma+i\left[\Omega+O\left(\frac{1}{\tau}\right)\right]$ on the curve corresponds to $\Omega^{(m)}=2\pi m\varepsilon$, $m=\pm1,\pm2,\pm3,\ldots$, $\varepsilon=1/\tau$. The fixed point is stable if the imaginary parts of the eigenvalues are outside of the interval $\Omega_1<\Omega<\Omega_2$. Such a case with $\Omega^{(m_0)}<\Omega_1<\Omega_2<\Omega^{(m_0+1)}$ is illustrated, in which the leading eigenvalues $\Lambda^{(m_0)}$ and $\Lambda^{(m_0+1)}$ have negative real parts.

IV. CONTROL DOMAIN CLOSE TO THE HOPF BIFURCATION

In this section, we show that strongly delayed feedback can stabilize a fixed point in the case when the fixed point is sufficiently close to the Hopf bifurcation. In our case, this means that λ is small. In particular, we are going to prove that the delayed feedback control scheme will be successful even for large delay within the range of order $1/\lambda^2$. We will also provide conditions for successful control.

For the fixed point that is close to the Hopf bifurcation, we assume $K>\lambda$, and hence it has an unstable PS, as shown in Fig. 2(e). As λ stays fixed, with increasing τ the curve of the PS will be densely filled with the eigenvalues $(\Omega^{(m)}=2\pi m/\tau)$. The only possibility for the fixed point to become stable is to assume that λ is also scaled with increasing τ. Particularly, we will show that in order to achieve control, we have to scale it as $\lambda=\lambda_0\varepsilon^2$ with fixed λ_0 (here, for convenience, we introduce the small parameter $\varepsilon=1/\tau$).

Figure 3 illustrates the part of the curve $\gamma(\Omega)$ which may induce an instability in the system. More precisely, the interval of unstable frequencies is $\Omega_1<\Omega<\Omega_2$, where Ω_1 and Ω_2 are given by the zeros of $\gamma(\Omega)$,

$$\Omega_{1,2}=\omega\pm K\sqrt{1-\left(1-\frac{\lambda}{K}\right)^2}.$$

For small λ, we can approximate this as

$$\Omega_{1,2} = \omega \pm \sqrt{2\lambda K}. \tag{6}$$

The length of the interval of unstable frequencies is $\Delta\Omega = \Omega_2 - \Omega_1 = 2\sqrt{2\lambda K}$.

We note that the actual position of the eigenvalues on the curve corresponds to the values of $\Omega^{(m)} = 2\pi m\varepsilon$ with any integer m. It is easy to see that the distance between the frequencies of neighboring eigenvalues $\Omega^{(m+1)} - \Omega^{(m)} = 2\pi\varepsilon$ scales as ε. Therefore, the control can be successful if $\lambda = \lambda_0\varepsilon^2$. In this case the length of the unstable interval is $\Delta\Omega = 2\varepsilon\sqrt{2\lambda_0 K}$ and scales also as ε. The control can be achieved if the length is smaller than the distance between neighboring eigenvalues, i.e., $\Delta\Omega = 2\varepsilon\sqrt{2\lambda_0 K} < 2\pi\varepsilon$, leading to

$$K < \frac{\pi^2}{2\lambda_0}. \tag{7}$$

Equation (7) gives a necessary condition for successful control.

The relative phase of the delay plays an additional important role. Depending on this phase, control occurs periodically with τ. In order to quantify this effect, let us introduce $\omega_\tau = 2\pi/\tau$ to be the frequency associated with the delay. Then the ratio of the internal frequency ω and ω_τ is given by $\omega/\omega_\tau = \gamma_\tau$ mod 1. Here $0 < \gamma_\tau < 1$ measures the detuning from the resonance between the internal frequency and the delay-induced one. Using this notation and Eq. (6), we can rewrite

$$\Omega_{1,2} = m_0\omega_\tau + \gamma_\tau\omega_\tau \pm \varepsilon\sqrt{2\lambda_0 K} = \Omega^{(m_0)} + \varepsilon(2\pi\gamma_\tau \pm \sqrt{2\lambda_0 K}).$$

Here m_0 is some integer number. The necessary and sufficient condition for the stability is (cf. Fig. 3) $\Omega^{(m_0)} < \Omega_1 < \Omega_2 < \Omega^{(m_0+1)}$, which leads to

$$\sqrt{2\lambda_0 K} < 2\pi \min\{\gamma_\tau, 1 - \gamma_\tau\}$$

or

$$K < \frac{2\pi^2}{\lambda_0}(\min\{\gamma_\tau, 1-\gamma_\tau\})^2 = \frac{2\pi^2}{\lambda_0}\left(\min\left\{\left[\frac{\omega\tau}{2\pi}\right]_f, 1 - \left[\frac{\omega\tau}{2\pi}\right]_f\right\}\right)^2, \tag{8}$$

where $\left[\frac{\omega\tau}{2\pi}\right]_f$ is the fractional part of $\frac{\omega\tau}{2\pi}$ [35]. Figure 4 shows the domain of control given by Eq. (8) for $\lambda = \lambda_0/\tau^2$.

In order to return to unscaled parameters, we have to substitute $\lambda_0 = \lambda/\varepsilon^2 = \lambda\tau^2$. Figure 5(a) shows the obtained domain of control for fixed small $\lambda = 0.01$. The maximum allowed values of K decrease as $1/\tau^2$. More precisely, we have

$$K_{\max}(\tau) = \frac{\pi^2}{2\lambda\tau^2}. \tag{9}$$

The application of the asymptotic analysis allows us to reveal many essential features and mechanisms of the stabilization control scheme (1) for large delay τ. On the other hand, the obtained approximations are valid as soon as K is much larger than λ. Figure 5 shows a comparison of the boundaries of the control domain, which are given by the asymptotic methods and exact analytical formulas derived in Appendix A. Very close to the Hopf bifurcation ($\lambda = 0.01$), the agreement is excellent even at small values of τ [Fig. 5(a)], while for larger λ [Fig. 5(b)] the deviations become more visible. In addition, the approximate solution does not give the lower boundary of the control domain for small K, which only shows up in Fig. 6. The analytical approach which we give in Appendix A also allows us to identify the "peaks" of the control domains, which occur at $\tau_{\max} = (2n+1)\pi/\omega$, $n = 0, 1, 2, \ldots$, as double-Hopf bifurcation points. The critical time delay, above which control fails, is given by $\tau_c = 2/\lambda$.

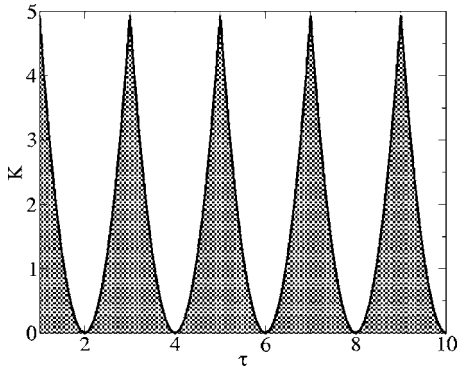

FIG. 4. Shaded region: Domain of control in the (τ, K) plane for the fixed point close to the Hopf bifurcation, given by the asymptotic formula Eq. (8) for $\lambda = \lambda_0/\tau^2$. Parameters: $\omega = \pi$, $\lambda_0 = 1$.

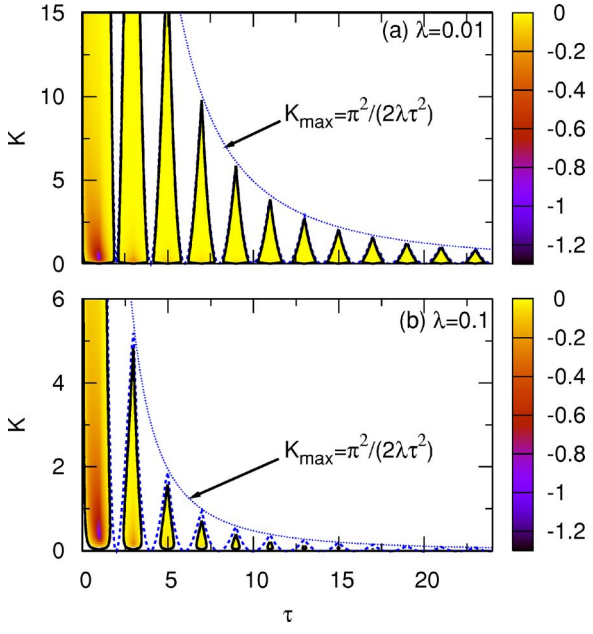

FIG. 5. (Color online) Domain of control in the (τ, K) plane, and largest negative real part of the complex eigenvalues $\Lambda(K, \tau)$ (in color code) calculated from the characteristic equation using the Lambert function [Eq. (3)]. Dashed lines (blue): asymptotic approximation Eq. (8) of stability boundary; dotted line (blue): approximate maxima Eq. (9). Solid lines: exact stability boundaries, cf. Eqs. (A3) and (A4). Parameters: (a) $\omega = \pi$, $\lambda = 0.01$, (b) $\omega = \pi$, $\lambda = 0.1$.

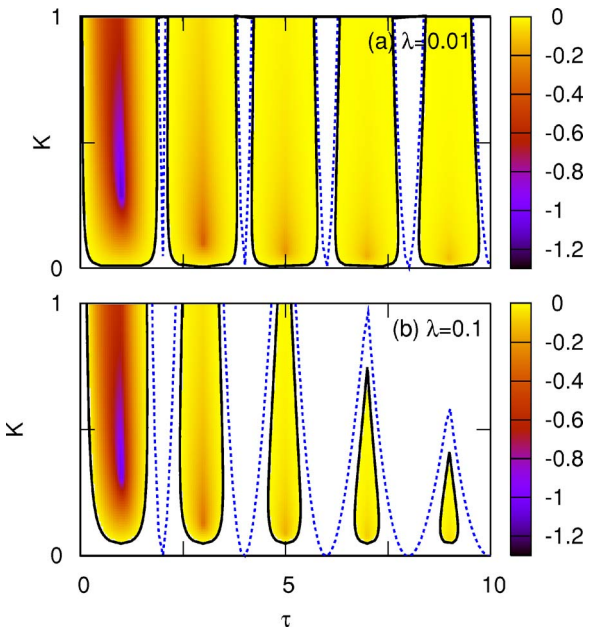

FIG. 6. (Color online) Enlargement of Fig. 5: Deviation of the asymptotic results (dashed) from the exact stability boundary (solid) for small K or large λ.

An inspection of the islands of stabilization in Figs. 5 and 6 reveals that the absolute value of the real part of the critical eigenvalue, i.e., the eigenvalue that has the largest real part (but remains negative within those islands), decreases with increasing τ. Hence the fixed point becomes less stable, and it is expected that the system becomes more sensitive to noise, and it will be more difficult to realize stabilization experimentally, if the delay time is chosen several times the system's characteristic time T_0.

V. CONCLUSIONS

Time delays occur naturally in a variety of optical, electronic, chemical, biological, and other nonlinear systems. This feature can be used in a simple and easily realizable way to stabilize unstable steady states by time-delayed difference feedback control. However, the control scheme may fail if the delay time τ and the control amplitude K are not chosen appropriately. In this paper, we have elaborated analytical conditions for successful control of a fixed point of focus type. By asymptotic expansion methods for large delay, and a detailed comparison with exact solutions, we have established the parameter ranges for successful control. Thereby we have not only obtained the precise shape of the islands of control in the (τ,K) parameter plane, but have also gained insight into the mechanism of control by analyzing the eigenvalue spectrum of the fixed point of the delay-differential equation, which consists of a pseudocontinuous spectrum and up to two strongly unstable complex eigenvalues. Although our analysis has shown that the standard control scheme generally fails for large delay, we have found that if the uncontrolled system is sufficiently close to its instability threshold, i.e., a Hopf bifurcation, control does work even for relatively large delay times, compared to the intrinsic oscillation period $T_0=2\pi/\omega$, cf. Fig. 5(a). These results may be of interest, e.g., in application to laser systems where oscillatory instabilities may occur above the first laser threshold, but stable cw operation is often desired [25]. By suitable optical or optoelectronic feedback using, for instance, external cavities and Fabry-Perot resonators, time-delayed feedback control may be realized.

ACKNOWLEDGMENTS

This work was supported by DFG in the framework of Sfb 555.

APPENDIX A: BOUNDARIES OF THE CONTROL DOMAIN

The exact boundaries of the control domain can be obtained analytically [19] from the characteristic Eq. (2) by setting the real part of the complex eigenvalue Λ equal to zero, i.e., $\Lambda=i\Omega$. We then obtain the two real equations

$$\lambda = K(1-\cos\Omega\tau), \tag{A1}$$

$$\pm\omega = \Omega + K\sin\Omega\tau. \tag{A2}$$

Solving this system of transcendental equations and observing the positivity of the delay time τ and the parameters λ,ω,K, we find three families of branches of solutions, where the non-negative integer n takes care of the different leaves of the involved multivalued functions,

$$\tau_1(K,n) = \frac{2n\pi + \arccos\dfrac{K-\lambda}{K}}{\omega - \sqrt{(2K-\lambda)\lambda}}, \quad \frac{\lambda}{2} \leqslant K < \frac{\omega^2+\lambda^2}{2\lambda}, \tag{A3}$$

$$\tau_2(K,n) = \frac{2(n+1)\pi - \arccos\dfrac{K-\lambda}{K}}{\omega + \sqrt{(2K-\lambda)\lambda}}, \quad \frac{\lambda}{2} \leqslant K, \tag{A4}$$

$$\tau_3(K,n) = \frac{2(n+1)\pi - \arccos\dfrac{K-\lambda}{K}}{-\omega + \sqrt{(2K-\lambda)\lambda}}, \quad \frac{\omega^2+\lambda^2}{2\lambda} < K. \tag{A5}$$

The corresponding eigenvalues $\Lambda=i\Omega$ are given by

$$\Omega_{1,3} = \pm[\omega - \sqrt{(2K-\lambda)\lambda}],$$

$$\Omega_2 = \pm[\omega + \sqrt{(2K-\lambda)\lambda}].$$

For the boundaries of the stability islands, only the branches τ_1 and τ_2 are relevant. Note that at the points

$$K = K_{\min} = \frac{\lambda}{2},$$

$$\tau = \tau_{\min}(n) = \frac{(2n+1)\pi}{\omega},$$

the branch $\tau_1(K,n)$ ends, but is continued by $\tau_2(K,n)$. As it is shown in [19], these pairs of curves, Eqs. (A3) and (A4), form the boundaries of the control domains in the (τ,K) parameter plane, as depicted by solid lines in Figs. 5 and 6. These islands become smaller for increasing n and the corresponding values for K are confined by

$$K_{\min} \leqslant K \leqslant K_{\max}(n),$$

where the maximal value $K_{\max}(n)$ is given by an intersection point of the two branches $\tau_1(K,n)$ and $\tau_2(K,n)$. These intersection points correspond to double-Hopf points of codimension 2. They are given by solutions of the transcendental equation

$$\arccos\frac{\lambda - K}{K} = \frac{(2n+1)\pi}{\omega}\sqrt{(2K-\lambda)\lambda}. \tag{A6}$$

The corresponding values of τ are given by

$$\tau_{\max}(n) = \tau_{\min}(n) = \frac{(2n+1)\pi}{\omega}. \tag{A7}$$

Note that the condition (A6) is satisfied also for $K=K_{\min}$. The stability domain vanishes if $K_{\min}$ and $K_{\max}$ coincide. Forming the derivative of Eq. (A6) with respect to K, we obtain

$$\frac{1}{K} = \frac{(2n+1)\pi}{\omega}.$$

Inserting $K=K_{\min}=\lambda/2$ finally gives the relation

$$\omega = \frac{(2n+1)\pi\lambda}{2}.$$

If this relation is satisfied, we have a resonant double-Hopf point of codimension 3. Since n has to be an integer, this happens only for particular choices of λ and ω. Otherwise, the integer part of the value n obtained from this relation gives the number of nondegenerate stability islands.

Using Eq. (A7), the maximum delay time τ_c which allows for stabilization is obtained as

$$\tau_c = \frac{2}{\lambda}.$$

Note that this boundary is sharp only if τ is an odd integer multiple of π/ω. For

$$\frac{\omega}{\lambda} < \frac{\pi}{2},$$

even the first stability island vanishes and stabilization is not possible.

[1] H. G. Schuster, *Handbook of Chaos Control* (Wiley-VCH, Weinheim, 1999).
[2] S. Boccaletti, C. Grebogi, Y. C. Lai, H. Mancini, and D. Maza, Phys. Rep. **329**, 103 (2000).
[3] D. Gauthier, G. M. Hall, R. A. Olivier, E. G. Dixon-Tulloch, P. D. Wolf, and S. Bahar, Chaos **12**, 952 (2003).
[4] E. Ott, C. Grebogi, and J. A. Yorke, Phys. Rev. Lett. **64**, 1196 (1990).
[5] K. Pyragas, Phys. Lett. A **170**, 421 (1992).
[6] J. E. S. Socolar, D. W. Sukow, and D. J. Gauthier, Phys. Rev. E **50**, 3245 (1994).
[7] A. Kittel, J. Parisi, and K. Pyragas, Phys. Lett. A **198**, 433 (1995).
[8] D. W. Sukow, M. E. Bleich, D. J. Gauthier, and J. E. S. Socolar, Chaos **7**, 560 (1997).
[9] K. Pyragas, Phys. Rev. Lett. **86**, 2265 (2001).
[10] N. Baba, A. Amann, E. Schöll, and W. Just, Phys. Rev. Lett. **89**, 074101 (2002).
[11] O. Beck, A. Amann, E. Schöll, J. E. S. Socolar, and W. Just, Phys. Rev. E **66**, 016213 (2002).
[12] I. Harrington and J. E. S. Socolar, Phys. Rev. E **69**, 056207 (2004).
[13] M. E. Bleich and J. E. S. Socolar, Phys. Lett. A **210**, 87 (1996).
[14] W. Just, T. Bernard, M. Ostheimer, E. Reibold, and H. Benner, Phys. Rev. Lett. **78**, 203 (1997).
[15] H. Nakajima, Phys. Lett. A **232**, 207 (1997).
[16] K. Pyragas, Phys. Rev. E **66**, 026207 (2002).
[17] C. von Loewenich, H. Benner, and W. Just, Phys. Rev. Lett. **93**, 174101 (2004).
[18] A. G. Balanov, N. B. Janson, and E. Schöll, Phys. Rev. E **71**, 016222 (2005).
[19] P. Hövel and E. Schöll, Phys. Rev. E **72**, 046203 (2005).
[20] S. Bielawski, M. Bouazaoui, D. Derozier, and P. Glorieux, Phys. Rev. A **47**, 3276 (1993).
[21] A. Chang, J. C. Bienfang, G. M. Hall, J. R. Gardner, and D. J. Gauthier, Chaos **8**, 782 (1998).
[22] K. Pyragas, V. Pyragas, I. Z. Kiss, and J. L. Hudson, Phys. Rev. Lett. **89**, 244103 (2002).
[23] K. Pyragas, V. Pyragas, I. Z. Kiss, and J. L. Hudson, Phys. Rev. E **70**, 026215 (2004).
[24] A. Ahlborn and U. Parlitz, Phys. Rev. Lett. **93**, 264101 (2004).
[25] J. Ohtsubo, *Semiconductor Lasers* (Springer, Berlin, 2005).
[26] *Unlocking Dynamical Diversity: Optical Feedback Effects on Semiconductor Lasers*, edited by D. M. Kane and K. A. Shore (Wiley VCH, Weinheim, 2005).
[27] *Fundamental Issues of Nonlinear Laser Dynamics*, AIP Conf. Proc. No. 548, edited by B. Krauskopf and D. Lenstra (American Institute of Physics, Melville, NY, 2000).
[28] S. Yanchuk, Math. Methods Appl. Sci. **28**, 363 (2005).
[29] I. Fischer, G. H. M. van Tartwijk, A. M. Levine, W. Elsäßer, E. Göbel, and D. Lenstra, Phys. Rev. Lett. **76**, 220 (1996).
[30] T. Heil, I. Fischer, W. Elsäßer, and A. Gavrielides, Phys. Rev. Lett. **87**, 243901 (2001).
[31] V. Z. Tronciu, H.-J. Wünsche, M. Wolfrum, and M. Radziunas, Phys. Rev. E **73**, 046205 (2006).

[32] J. K. Hale, *Functional Differential Equations*, Applied Mathematical Sciences Vol. 3 (Springer, New York, 1971).

[33] S. Yanchuk and M. Wolfrum, in *Proceedings of the 5th EUROMECH Nonlinear Dynamics Conference ENOC-2005, Eindhoven*, edited by D. H. van Campen, M. D. Lazurko, and W. P. J. M. van den Oever (Eindhoven University of Technology, Eindhoven, The Netherlands, 2005), pp. 08–010.

[34] S. Lepri, G. Giacomelli, A. Politi, and F. T. Arecchi, Physica D **70**, 235 (1994).

[35] Practically, one has also to satisfy $K>\lambda$, but our scaling assumes the smallness of λ.